Biomedicine & Pharmacotherapy 177 (2024) 116881

Contents lists available at ScienceDirect

Biomedicine & Pharmacotherapy

journal homepage: www.elsevier.com/locate/biopha

Photodynamic therapy offers a novel approach to managing miltefosine-resistant cutaneous leishmaniasis

Fernanda V. Cabral [a], Mina Riahi [b], Saydulla Persheyev [b], Cheng Lian [b], Mauro Cortez [c], Ifor D. W. Samuel [b,*], Martha S. Ribeiro [a,**]

[a] Center for Lasers and Applications, Nuclear and Energy Research Institute (IPEN-CNEN), São Paulo, Brazil
[b] Organic Semiconductor Centre, SUPA, School of Physics and Astronomy, University of St Andrews, St Andrews, KY16 9SS, UK
[c] Institute of Biomedical Sciences, University of São Paulo (ICB/USP), São Paulo, SP, Brazil

ARTICLE INFO

Keywords:
1,9-dimethyl-methylene blue (DMMB)
Leishmania amazonensis
Organic light emitting-diodes (OLEDs)
Antimicrobial resistance
Wearable light sources

ABSTRACT

Cutaneous leishmaniasis (CL) is a neglected disease caused by *Leishmania* parasites. The oral drug miltefosine is effective, but there is a growing problem of drug resistance, which has led to increasing treatment failure rates and relapse of infections. Photodynamic therapy (PDT) combines a light source and a photoactive drug to promote cell death by oxidative stress. Although PDT is effective against several pathogens, its use against drug-resistant *Leishmania* parasites remains unexplored. Herein, we investigated the potential of organic light-emitting diodes (OLEDs) as wearable light sources, which would enable at-home use or ambulatory treatment of CL. We also assessed its impact on combating miltefosine resistance in *Leishmania amazonensis*-induced CL in mice. The *in vitro* activity of OLEDs combined with 1,9-dimethyl-methylene blue (DMMB) (OLED-PDT) was evaluated against wild-type and miltefosine-resistant *L. amazonensis* strains in promastigote (EC_{50} = 0.034 μM for both strains) and amastigote forms (EC_{50} = 0.052 μM and 0.077 μM, respectively). Cytotoxicity in macrophages and fibroblasts was also evaluated. *In vivo*, we investigated the potential of OLED-PDT in combination with miltefosine using different protocols. Our results demonstrate that OLED-PDT is effective in killing both strains of *L. amazonensis* by increasing reactive oxygen species and stimulating nitric oxide production. Moreover, OLED-PDT showed great antileishmanial activity *in vivo*, allowing the reduction of miltefosine dose by half in infected mice using a light dose of 7.8 J/cm^2 and 15 μM DMMB concentration. In conclusion, OLED-PDT emerges as a new avenue for at-home care and allows a combination therapy to overcome drug resistance in cutaneous leishmaniasis.

1. Introduction

Leishmaniasis is a neglected and poverty-related disease caused by protozoa parasites of the genus *Leishmania*, which has two major clinical forms: visceral and cutaneous. The cutaneous forms normally involve ulcerated lesions at the site of infection, which may significantly lead to mental illness and psychosocial morbidity, affecting the quality of life of patients [1]. Its treatment comprises highly toxic formulations of intravenous or intramuscular administration for a long period, which are expensive, and sometimes unaffordable for patients [2]. Consequently, there is a poor adherence of patients to treatments, hence contributing to treatment failure and selection of resistant phenotypes [3].

The emergence of drug resistance in leishmaniasis has been a major concern in recent years [3]. The limited treatment options and widespread misuse of drugs have created a sense of urgency for the development of effective therapies to address this problem. Miltefosine (MF), for example, is approved for the treatment of cutaneous leishmaniasis (CL) in many countries worldwide, including India, Argentina, Israel, USA and others [4]. It is also included in the World Health Organization's list of essential medicines, indicating its widespread use and importance in healthcare systems globally [5]. Moreover, MF offers some advantages in the treatment of cutaneous leishmaniasis, such as: i-) oral administration; ii-) high efficacy as MF can be effective in treating various forms of CL; and iii) broad-spectrum activity against multiple species of *Leishmania* parasites, making it useful in regions where different species may be prevalent. However, MF also has some drawbacks and harmful effects, including: i) adverse reactions such as

* Correspondence to: North Haugh, St Andrews, Fife, KY16 9SS, UK.
** Correspondence to: Av. Lineu Prestes, 2242, São Paulo, SP 05508-000, Brazil.
E-mail addresses: idws@st-andrews.ac.uk (I.D.W. Samuel), marthasr@usp.br (M.S. Ribeiro).

https://doi.org/10.1016/j.biopha.2024.116881
Received 15 March 2024; Received in revised form 26 May 2024; Accepted 3 June 2024
Available online 24 June 2024

nausea, vomiting, and diarrhea; ii) teratogenicity; and iii) development of resistance [5].

This combination of benefits and drawbacks highlights the need for ongoing research and development of new strategies against CL. Additionally, due to the rapid rise in treatment failure and refractory cases, combination regimens are preferred [6]. Therefore, the use of MF in combination with other therapies has been increasingly recommended [7]. Drug combinations may shorten the duration of treatment, improve compliance, enhance therapeutic efficacy, reduce costs and side effects, and prevent the emergence of resistance [7].

In this regard, photodynamic therapy (PDT) arises as a potential strategy to treat CL. PDT uses light to active a photosensitive drug that leads to the generation of reactive oxygen species (ROS) to kill cells by oxidative stress [8]. Although PDT is widely used in cancer treatment, it

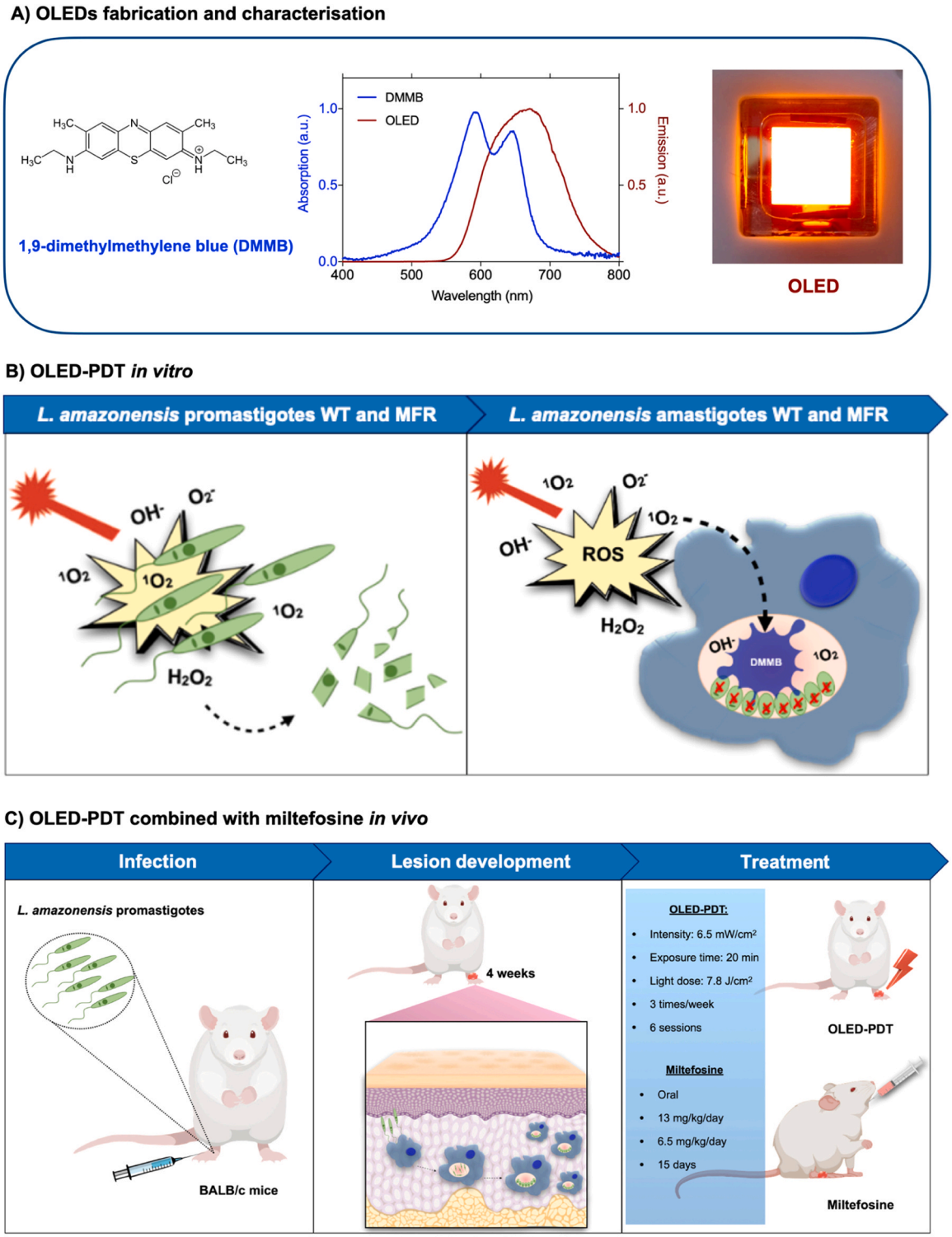

Fig. 1. Schematic illustration of the experimental design. (A) OLEDs were fabricated to match the absorbance of the PS DMMB. (B) *In vitro* activity of OLED-PDT against promastigotes and intracellular amastigotes of the WT and MFR strains of *L. amazonensis*. (C) *In vivo* activity of OLED-PDT alone and in combination with MF on BALB/c mice infected by *L. amazonensis*.

represents a promising strategy for treating localized infectious diseases since it possesses broad-spectrum activity and effective killing of resistant pathogens [9]. Besides, because of its multi-target features, it can oxidize different cellular biomolecules, thereby preventing the selection of resistant microorganisms. As a topical treatment, PDT offers further benefits, including targeting pathogens directly to the site of infection without significant toxicity, thus accelerating wound healing [10]. Yet, PDT has demonstrated synergy with antibiotics and antifungals in *in vitro* studies [11–13].

Different photoactive compounds have been used to mediate PDT [9–13]. Phenothiazinium derivatives, such as methylene blue (MB), are cationic molecules that increase their interaction with negatively charged biological membranes compared to anionic or neutral compounds. MB analogues, *e.g.*, 1,9- dimethyl methylene blue (DMMB), have emerged as promising alternatives to MB due to their augmented lipophilicity [14]. Moreover, DMMB exhibits the ability to generate 21 % more singlet oxygen than MB, further enhancing PDT efficacy [14, 15].

In addition to the photosensitisers (PSs), different light sources, such as lasers and LEDs (light-emitting diodes), have been broadly explored in PDT. Despite their benefits, they are bulky devices available in a limited number of clinical settings. Organic LEDs (OLEDs), however, are widely studied for use in displays and lighting, but there is a growing realization that their distinctive properties can open new fields of application, including biology and medicine [16–18]. They are very unusual and attractive light sources for medical applications because they are thin and lightweight, emit light over an area, and can be flexible. Yet, their emission can be tuned, their energy of manufacture is low and they are expected to be cost-effective when mass-produced. The use of OLEDs may be particularly beneficial for CL, as they are flexible and wearable light sources. They are suitable for at-home use or ambulatory treatment, hence enabling patient compliance.

Here we hypothesise that PDT combined with MF can be an innovative approach for targeted therapy and tackle antileishmanial drug resistance. We show that OLEDs combined with DMMB (OLED-PDT) can be effective in inactivating *Leishmania* parasites, including drug-resistant species. We engineered red OLEDs to match the absorbance of DMMB and evaluated OLED-PDT on both wild-type and MF-resistant (MFR) strains, encompassing both promastigotes and intracellular amastigotes forms of *Leishmania amazonensis*. This species is also responsible for the diffuse clinical manifestation of CL. Moreover, we take an important step towards translation to the clinic by conducting pioneering animal studies of OLED-PDT combined with MF to address drug resistance in CL induced in mice (Fig. 1).

2. Material and methods

2.1. Parasites

Promastigotes of *L. amazonensis WT* (MHOM/BR/73/M2269) were grown at 28°C in M199 medium (Sigma-Aldrich, USA), HEPES (0.04 M) pH 7.4 (Sigma-Aldrich, USA), hemin (2.5 $mgmL^{-1}$) (Sigma-Aldrich, USA) and adenosine (0.01 M) (Sigma-Aldrich, USA) supplemented with 10 % heat-inactivated fetal bovine serum (FBS; Gibco™ Invitrogen Corporation). The *L. amazonensis* MFR was selected from the reference strain M2269 (MF 150.3–1 line) as described elsewhere [19]. MFR parasites were grown in the presence of MF (0.15 M) (Sigma-Aldrich, USA), in the same media as the WT line. *L. amazonensis* transgenic line expressing luciferase was also obtained from the reference strain M2269 and grown in the same conditions as the other strains. Transfected parasites were selected in the presence of hygromycin (32 μgml^{-1}) [20]. At least two independent experiments were performed in triplicate.

2.2. OLED fabrication

OLEDs were fabricated by a thermal evaporator (EvoVac, Angstrom Engineering Inc.) at a base pressure of 3×10^{-7} mbar. Two different sizes of OLEDs were made: 3.2 cm by 4.1 cm for *in vitro* studies and 1.4 cm by 1.4 cm for *in vivo* studies. The OLEDs were designed in a top-emitting configuration using a 150 nm Al bottom electrode deposited on a glass substrate at 3 Å/s. A hole transport layer consisting of 40 nm 2,2′,7,7′-tetra (N, N-di-p-tolyl) amino-9,9-spirobifluorene (Spiro-TTB) p doped by 2,2-(-(perfluoronaphthalene-2,6-diylidene) dimalononitrile (F6-TCNNQ) (4 wt%) was then deposited at 0.6 Å/s. 10-nm of NPB (N, N′-bis (naphthalen-1-yl)-N,N′-bis(phenyl)-benzidine) was then deposited as an electron blocking layer. A 40 nm 10 wt% $Ir(MDQ)_2(acac)$ (2-methyldibenzo[*f*,*h*]quinoxaline)(acetylacetonate)iridium(III)- doped NPB was used as the emissive layer and deposited at 0.3 Å/s. Then a 10 nm hole-blocking layer consisting of bis(8-hydroxy-2-methyl quinoline) -(4-phenylphenoxy) aluminium (BAlq) was deposited at 0.3 Å/s. Then a 60 nm n doped electron transport layer of cesium-doped 4,7-diphenyl-1,10- phenanthroline (BPhen) was deposited at 1 Å/s, followed by 20 nm silver as a top electrode, and 80 nm NPB capping layer to improve outcoupling efficiency.

2.3. OLED-PDT activity against WT and MFR L. amazonensis promastigotes

L. amazonensis promastigotes of the WT and MFR strains were seeded at a density of 1×10^6 parasites per well into a 96-well plate. OLED-PDT activity against both strains was conducted by the addition of serial dilutions of DMMB (0–3 μM) (Sigma-Aldrich, USA), incubated for 10 min before irradiation. Parasites were treated with a red OLED giving broad emission peaking at 670 nm. An irradiance of 6.5 $mWcm^{-1}$ was applied for 20 min, giving a light dose of 7.8 Jcm^{-2}. The cellular viability of parasites was carried out by the addition of resazurin (10 μL at 1.1 $mgml^{-1}$) (Sigma-Aldrich, USA), incubated for 4 h. The fluorescence intensity was then measured by using a microplate reader (Spectramax M4, Molecular Devices, USA) at $\lambda_{ex} = 530$ nm and $\lambda_{em} = 590$ nm. Results were normalized and plotted as a percentage of live parasites. The effective concentration of DMMB to kill 50 % (EC_{50}) and 90 % (EC_{90}) of parasites against both strains treated by OLED-PDT at 7.8 Jcm^{-2} was determined by sigmoidal regression analysis using GraphPad Prism 7.0 software.

Fluorescence microscopy of promastigotes was assessed by live/dead staining assay after OLED-PDT according to the instructions of the manufacturer. Briefly, parasites were treated with DMMB concentration equivalent to the EC_{90} of each strain, delivering a light dose of 7.8 Jcm^{-2}. Parasites were then washed and stained with live/dead kit assay (Sigma-Aldrich, USA) for 15 min. Images were acquired with a fluorescence microscope (Nikon, Japan) and analysed by ImageJ software (https://imagej.nih.gov/ij/plugins/cell-counter.html).

2.4. ROS detection assay on promastigotes treated by OLED-PDT

L. amazonensis promastigotes WT and MFR were seeded into 96-well plates (1×10^6 per well). Parasites were illuminated by the red OLED at 7.8 Jcm^{-2} and incubated with a DMMB concentration corresponding to the EC_{90} determined for each strain (0.224 and 0.256 μM, for the WT and MFR, respectively). Untreated cells were used as a negative control and H_2O_2 (0.1 mM) as a positive control. ROS production was obtained by using a fluorescent indicator 2′-7′-dichlorodihydrofluorescein diacetate (DCFH-DA) (Sigma-Aldrich, USA). After OLED-PDT, DCFH-DA (10 μM) was added to each well and incubated for 45 min. Fluorescence intensity was detected by using a microplate reader (Spectramax M4, Molecular Devices, USA) at $\lambda_{ex} = 485$ nm and $\lambda_{em} = 535$ nm.

2.5. In vitro cytotoxicity assay

2.5.1. OLED-PDT cytotoxicity on mammalian cells

Mouse embryonic fibroblast cells (NIH 3T3) were harvested in

DMEM medium (15 mM HEPES, 2 g of sodium bicarbonate.L^{-1}, and 1 mM L-glutamine) and supplemented with 10 % FBS. Mouse RAW 264.7 macrophage cells were grown in RPMI 1640 medium (15 mM HEPES, 2 g of sodium bicarbonate/L, and 1 mM of L-glutamine) and supplemented with 10 % FBS. Both cell lines were incubated at 37°C and 5 % CO_2 atmosphere.

Cytotoxicity assay was assessed by evaluating the mitochondrial activity of both fibroblasts and macrophages seeded at a density of 5×10^3 and 8×10^4, respectively. Cells were allowed to adhere to 96-well plates overnight. Before irradiation cells were incubated for 10 min (pre-irradiation time) with different concentrations of DMMB (from 0 to 3 μM) to allow its uptake. Then, cells were irradiated using a red OLED (670 ± 140 nm) in an irradiance of 6.5 $mWcm^{-2}$, delivering 3 different radiant exposures (2, 4, and 7.8 Jcm^{-2}). Cytotoxicity of DMMB without light was also evaluated by exposing cells with the same concentrations of DMMB in the dark for the same period.

MF cytotoxicity was evaluated on RAW 264.7 macrophages. For this, 8×10^4 cells were seeded on 96-well plates 24 h prior to experiments. MF activity was performed by the addition of serial dilutions of MF (0–500 μM), for 24 h at 37°C and 5 % CO_2 atmosphere.

Cell viability was determined by MTT (3-[4,5-dimethyl-2-thiazolyl]-2,5-diphenyl-2 H-tetrazolium bromide) assay. Briefly, the cells were incubated with MTT (30 μL at 5 $mgmL^{-1}$; Sigma-Aldrich, USA) after treatment and maintained at 37°C for 4 h. Then, dimethyl sulfoxide (30 μL) was added to each well and the optical density was measured by using a spectrophotometer (Spectramax M4, Molecular Devices, USA) at 595 nm using a reference wavelength of 690 nm. Results were expressed as a percentage of live fibroblasts or macrophages and compared to the control. The cytotoxic concentration for 50 % of macrophages (CC_{50}) treated by either OLED-PDT or MF was obtained by sigmoidal regression analysis using GraphPad Prism 7.0 software.

Fluorescence microscopy was also conducted to investigate the morphology of cells after OLED-PDT treatment. For this, 2×10^5 fibroblasts or macrophages were allowed to adhere onto round glass coverslips placed to the bottom of 24-well plates, for 24 h. Cells were treated by OLED-PDT at the highest light dose (7.8 Jcm^{-2}) and the DMMB concentration used was 1.5 μM, which was found to be a non-toxic concentration for both mammalian cells. Cells were fixed with methanol, washed 3 times with PBS, and coverslips were incubated for 10 min with 2 μgml^{-1} of 4′,6-diamidino-2-phenylindole (DAPI, Sigma-Aldrich, USA). Images were acquired with a fluorescence microscope (Nikon, Japan) and processed by the ImageJ software.

2.5.2. OLED-PDT and miltefosine activity on intracellular amastigotes of WT and MFR L. amazonensis

Macrophages at a density of 2×10^5 were plated on round glass coverslips into 24-well plates 24 h before experiments. Cells were infected with promastigotes of both strains at stationary growth phase at a multiplicity of infection = 10 for 4 h, at 34°C. After that, infected cells were washed to remove non-internalized parasites and incubated in a fresh medium overnight. Then intracellular amastigotes were treated with either MF (0–50 μM) or OLED-PDT at 7.8 Jcm^{-2} and varying DMMB concentrations (0–0.75 μM).

After 24 h cells were fixed with methanol, washed with PBS, and stained with Giemsa. Then intracellular parasites were counted using optical microscopy. Results were determined by counting 100 cells per coverslip and expressed as a percentage of infected macrophages and the average number of amastigotes per infected macrophage. The infection index was calculated as follows:

$$\frac{\text{Number of amastigotes}}{\text{Number of infected macrophages}} \text{x \% infection}$$

The selectivity index (SI) was determined by the ratio between CC_{50} for macrophages and EC_{50} of either MF or DMMB when parasites were exposed to a light dose of 7.8 Jcm^{-2} as follows:

$$SI = \frac{CC_{50}}{EC_{50}}$$

2.5.3. ROS and NO detection on intracellular amastigotes treated by OLED-PDT

Macrophages were seeded and infected as outlined above. Afterward, WT and MFR intracellular amastigotes were treated with OLED-PDT at 7.8 Jcm^{-2} and incubated with the DMMB concentration corresponding to the EC_{50} (WT = 0.052 μM, MFR = 0.077 μM) and EC_{90} (WT = 0.47 μM, MFR = 0.31 μM) determined for each strain. Untreated infected macrophages were used as a negative control and H_2O_2 at 0.1 mM as a positive control.

ROS production was obtained with the same methods used for promastigotes as previously mentioned. After OLED-PDT, DCFH-DA (10 μM) was added to each well and incubated for 45 min. Fluorescence intensity was detected by using a microplate reader (Spectramax M4, Molecular Devices, USA) at λ_{ex} = 485 nm and λ_{em} = 535 nm.

To assess cellular NO levels, macrophages infected with amastigotes of both strains were treated with OLED-PDT under the same conditions described above. NO production was obtained by the addition of 10 μM of 4-amino-5-methylamino-2′,7′-difluorofluorescein (ThermoFisher, USA). Then, fluorescence intensity was detected by taking reads every 5 min over a 12 h period using a microplate reader (Spectramax M4, Molecular Devices, USA) at λ_{ex} = 495 nm and λ_{em} = 515 nm.

2.6. Analysis of OLED-PDT and MF in vivo

Animal experimentation was approved by the Ethical Committee on Animal Use from IPEN-CNEN under protocol number 280/21. Female BALB/c mice (6–8 weeks old) were infected in the left hind paw by injection of 10^6 stationary growth phase promastigotes of *L. amazonensis* expressing the luciferase gene. Disease progression was monitored for 4 weeks until the development of lesions was observed. After 4 weeks, animals were treated with OLED-PDT, MF, or a combination of both as outlined below. *In vivo* experiments were conducted in two phases.

2.6.1. OLED-PDT in vivo

In phase 1, we evaluated the *in vivo* potential of OLED-PDT using the same light parameters tested *in vitro* (7.8 Jcm^{-2}, 6.5 $mWcm^{-2}$, 20 min of exposure time). DMMB concentration was determined based on the results obtained from our *in vitro* cytotoxicity assays. We found that at a 1.5 μM concentration, macrophages and fibroblasts were still viable. Therefore, 8 animals were infected and randomly sorted into 2 groups (n = 4 per group), one untreated control and the other treated with OLED-PDT (OLED-PDT 1.5).

2.6.2. OLED-PDT combined with miltefosine in vivo

In phase 2, 20 BALB/c mice were infected and randomly sorted into 5 groups (n = 4 per group), **(1) Control:** Animals were infected and untreated, **(2) OLED-PDT 15**: In this group, DMMB concentration was increased by 10 times (15 μM), however light parameters remained unchanged, being the same as used *in vitro* and *in vivo* (phase 1). **(3) 6.5 MF**: The *in vivo* activity of MF at a half-dose (6.5 mg/kg/day) was evaluated **(4) OLED-PDT 15 + 6.5 MF:** Animals were treated with a dual therapy - OLED-PDT for 20 min at 7.8 Jcm^{-2} and DMMB at 15 μM associated with the half dose of MF 6.5 mg/kg/day, **(5) 13 MF:** Animals were treated with the top dose of MF (13 mg/kg/day) [19].

2.6.3. Treatment and disease progression

In phase 1**,** animals were anaesthetized with isoflurane (2.5 % induction and 1.5 % maintenance), and DMMB (30 μL) at 1.5 μM diluted in PBS was injected into the infected paw. DMMB was incubated for 10 min before illumination to allow its uptake by parasites. Animals from the group OLED-PDT 1.5 were treated with 6 sessions of PDT on alternate days in the first 2 weeks, starting on day 0. The last PDT session was carried out at the end of the second week (day 11).

In phase 2, mice from the OLED-PDT 15 group received a higher DMMB concentration, while the same light parameters and the number

of PDT sessions were applied. In the other 3 treated groups with MF, the drug was given orally by gavage daily for 15 days, starting on day 0.

Disease progression was monitored by assessing parasite burden, lesion thickness, and pain score for the following 21 days. Parasite burden was measured in real-time by the detection of luciferase activity through bioluminescence imaging (IVIS Spectrum, Caliper Life Sciences, USA). Before treatment, imaging was carried out to determine the presence and establish the baseline of parasite burden in all animals. Bioluminescence imaging was performed weekly and in the last PDT session of every week, corresponding to days 4,7,11,14, and 21 as shown in Fig. 2

For *in vivo* luminescence detection and imaging, 100 μL of luciferin (VivoGlo, Promega Corporation, USA) at 75 mg/kg was intraperitoneally injected in each animal. Afterwards, mice were anaesthetized with isoflurane (2.5 % induction and 1.5 % maintenance). Twenty minutes after luciferin administration, images were acquired using 2 min of exposure time in a high-resolution mode [21]. Total photon emission was evaluated by determining a region of interest and quantified through software (Caliper Life Sciences). The bioluminescent signal was expressed as photons/second/cm^2 /steradian (ph/sec/cm^2/sr).

Pain evaluation was performed using the von Frey test, which allows the assessment of nociceptive sensitization after mechanical stimulation. The von Frey test consists of 5 filaments with different gauges or stiffness. Each filament employs a different weight (weights of 10, 26, 60,

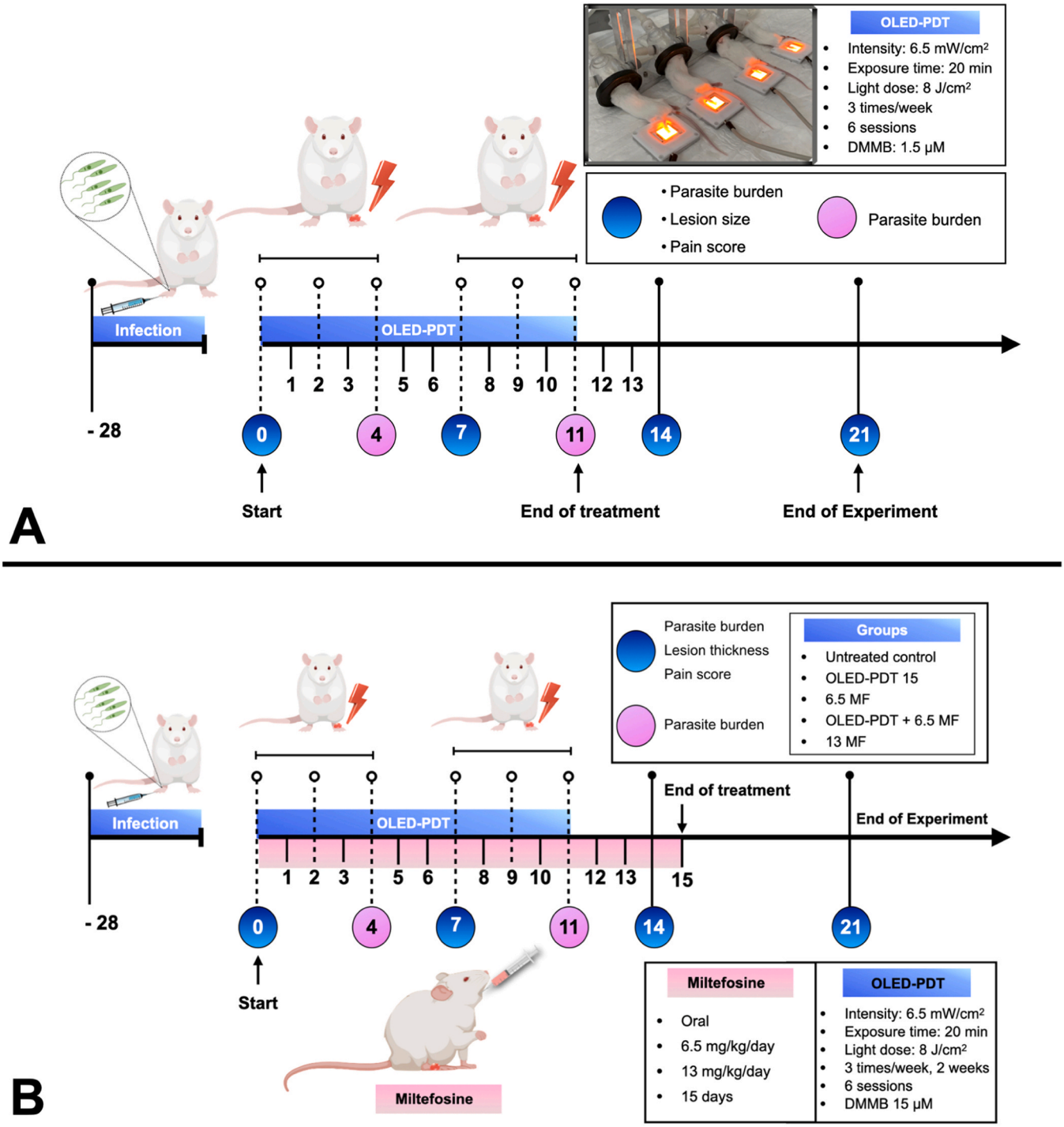

Fig. 2. Schematic illustrations of the *in vivo* experimental design of (A) OLED-PDT and (B) OLED-PDT combined or not with MF.

and 100 g) that is applied to the paw (from the weakest to the strongest) until the stimulus causes a paw withdrawal or a hind leg retraction [22]. A pain score was defined ranging from 1 to 6, in which 1 refers to the lowest nociceptive sensibility and 6 corresponds to the strongest response (severe pain) as shown in Table 1. Results were normalized and plotted as percentages.

Pain and lesion thickness were evaluated every week on days 0,7,14 and 21 (Fig. 2). Lesion thickness was determined by measuring the differences between infected and contralateral non-infected paw with a caliper as follows: Lesion thickness = Pi-Pc, in which Pi indicates the infected paw and Pc refers to the contralateral uninfected paw of the same animal [21].

2.7. Statistical analysis

Statistical analysis was evaluated using GraphPad Prism 7.0 software by one-way ANOVA, followed by the Tukey post-test. *In vitro* dose-response curves and *in vivo* statistical analysis were measured by two-way ANOVA followed by the Bonferroni post-test. Differences were considered statistically significant when $p < 0.05$.

3. Results

3.1. In vitro evaluation of OLED-PDT against the WT and MFR promastigotes of L. amazonensis

To assess the potential of OLED-PDT against promastigotes of the WT and MFR strains, DMMB was incubated at different concentrations 10 min before irradiation to allow the PS uptake by parasites. Then, an irradiance of 6.5 $mWcm^{-2}$ was applied for 20 min, giving a light dose of 7.8 Jcm^{-2}. The results show that either the WT or the resistant line of promastigotes were successfully killed even at the lowest DMMB concentration. The killing rate was increased at greater PS concentrations in a concentration-dependent manner. By doing a non-linear regression analysis we found that both lines showed a similar EC_{50} value of 0.034 μM, while a minor difference in the EC_{90} was noticed between both lines, equivalent to 0.22 μM and 0.25 μM, for the WT and MFR, respectively, with no statistically significant differences between strains (Fig. 3A).

To investigate whether those differences were related to ROS production, we measured the levels of ROS by exposing parasites to the same light conditions and DMMB concentration corresponding to the EC_{90} of each strain. ROS levels were substantially increased by 2.9-fold and 2.7-fold after OLED-PDT treatment, whereas H_2O_2 produced only 10.3 % and 17.9 % more ROS compared to untreated control for the WT and MFR, respectively (Fig. 3B). Nevertheless, no significant differences were noticed between the two strains, meaning that they were equally susceptible to our treatment under the experimental conditions. This susceptibility was further confirmed by fluorescence microscopy, which revealed that after OLED-PDT, parasites were almost completely killed. In Fig. 3**C** we observed only a few live parasites (stained with green-fluorescent dye), while nearly all promastigotes were dead (stained with red-fluorescent dye) after treatment.

Table 1
Pain score for Von Frey filaments referred to force scale.

Pain Score	Weight [g]
1	>100
2	60–100
3	26–60
4	15–26
5	10–15
6	<10

3.2. OLED-PDT is not toxic to mammalian cells

Our results demonstrate that DMMB did not promote cytotoxic effects on NIH 3T3 fibroblasts when incubated in the dark, regardless of the PS concentration (Fig. 4A). However, changes in mitochondrial activity were noticed when cells were treated with OLED-PDT. Differences in cellular viability were observed according to the light dose as well as the PS concentration. The lowest light doses (2 and 4 Jcm^{-2}) resulted in a slight reduction in fibroblast viability for concentrations greater than 0.75 μM. However, we demonstrate that 75 % of cells still were viable even at higher PS concentrations (Fig. 4B and C). By exposing the cells to the highest light dose (7.8 Jcm^{-2}), 88 % of cells were viable at 0.375 μM, whereas at the highest concentrations and same light dose, we observed 75 % of cellular metabolic activity (Fig. 4D).

Regarding the macrophages, no cytotoxicity was observed for DMMB in the dark, regardless of its concentration (Fig. 4E). We also noticed alterations in cellular viability when macrophages were treated by OLED-PDT as we increased the light dose and/or the DMMB concentration. Interestingly, at 0.75 μM no reduction in mitochondrial activity was observed at all light doses used, suggesting macrophages are more resistant to oxidative stress when compared to fibroblasts, except for the highest concentration (Fig. 4F, G, and H). Nonetheless, regardless of the cell line, in all treated groups either fibroblasts or macrophages were properly adhered to the bottom of the well plate. Yet, no morphological alterations were observed by fluorescence microscopy, as shown in Figs. 4I and 4J.

Cytotoxic evaluation of MF on macrophages was assessed by the addition of varying drug concentrations ranging from 0 to 500 μM. As a result, we also observed a dose-dependent effect of MF on macrophage viability **(**Fig. 4**K)**. By carrying out a sigmoidal regression analysis we calculated CC_{50} of MF and DMMB on macrophages. We found that the CC_{50} value of MF was 46.5 μM, while for DMMB, the CC_{50} value found corresponded to a concentration of around 1.2 μM for the highest light dose (7.8 Jcm^{-2}) (Fig. 4K).

3.3. Intracellular L. amazonensis WT and MFR amastigotes are highly susceptible to OLED-PDT

To evaluate the potential of OLED-PDT against the intracellular amastigotes, macrophages were infected with promastigotes of *L. amazonensis* WT and MFR at a multiplicity of infection of 10:1. After 24 h, parasites were treated with either OLED-PDT or MF. The experimental conditions used were set from the previous results reported and determined according to macrophages' cytotoxicity assay.

Infected macrophages were treated with a radiant exposure of 7.8 Jcm^{-2} and DMMB concentrations ranging from 0.96 to 0.75 μM since these concentrations were not toxic to these cells. In terms of the percentage of infection, our results show that macrophages were considerably infected by amastigotes, resulting in approximately 80 % of cells being infected by amastigotes of both strains. When parasites were treated with OLED-PDT, we noticed that at a very low nanomolar concentration (0.96 μM) the percentage of infection was significantly reduced to 47 % and 38 % in WT and MFR, respectively, in comparison with their respective untreated controls. At 0.75 μM, a further reduction of 49 % (WT) and 51 % (MFR) was observed (Fig. 5A and D).

In contrast, parasites treated with MF did not show a significant improvement in the percentage of infection. Since MF was toxic to macrophages at high concentrations (CC_{50} = 46.5 μM), the top concentration assigned was 50 μM. Therefore, under these conditions, the percentage of infection was reduced by only 16 % for the WT strain.

Untreated controls also presented similar numbers of intracellular amastigotes, accounting for an average of 15.7 and 12.3 parasites per infected macrophage for the WT and MFR lines, respectively. The number of amastigotes per infected macrophage was tremendously reduced by OLED-PDT, thus indicating a concentration-dependent activity against both strains. Surprisingly, even at the lowest

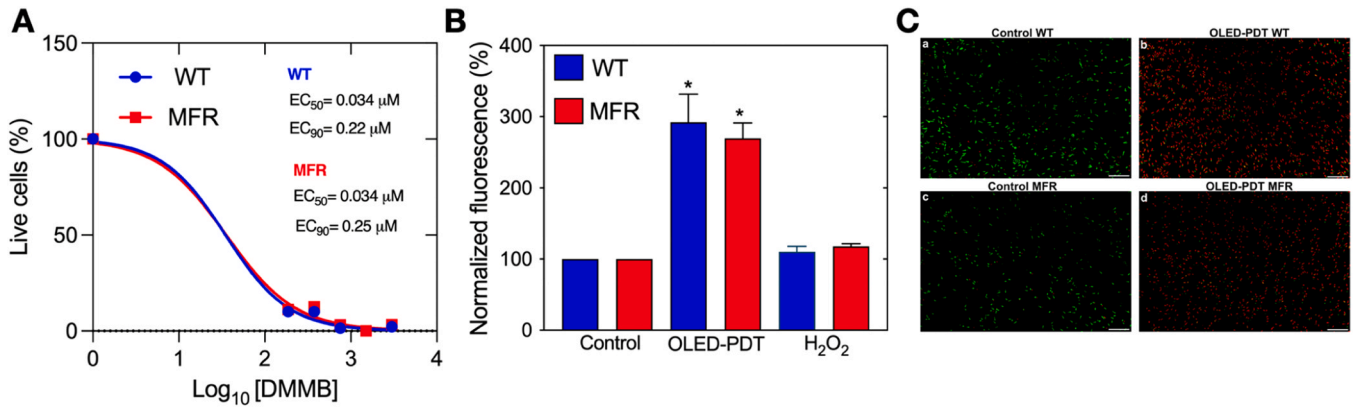

Fig. 3. *In vitro* activity of OLED-PDT against promastigotes of WT and MFR *L. amazonensis.* (A) Dose-response curve of the WT and MFR *L. amazonensis* promastigotes treated with OLED-PDT at 7.8 Jcm^{-2}, incubated with varying concentrations of DMMB; (B) ROS detection after OLED-PDT and DMMB concentration corresponds to the EC_{90} values of each strain. Dara are presented as mean values ± standard error ot the mean (SEM). *denotes statistically significant differences between treated groups and control; (C) Fluorescence microscopy images of promastigotes assessed by live/dead staining assay after OLED-PDT. Scale bar = 50 μm.

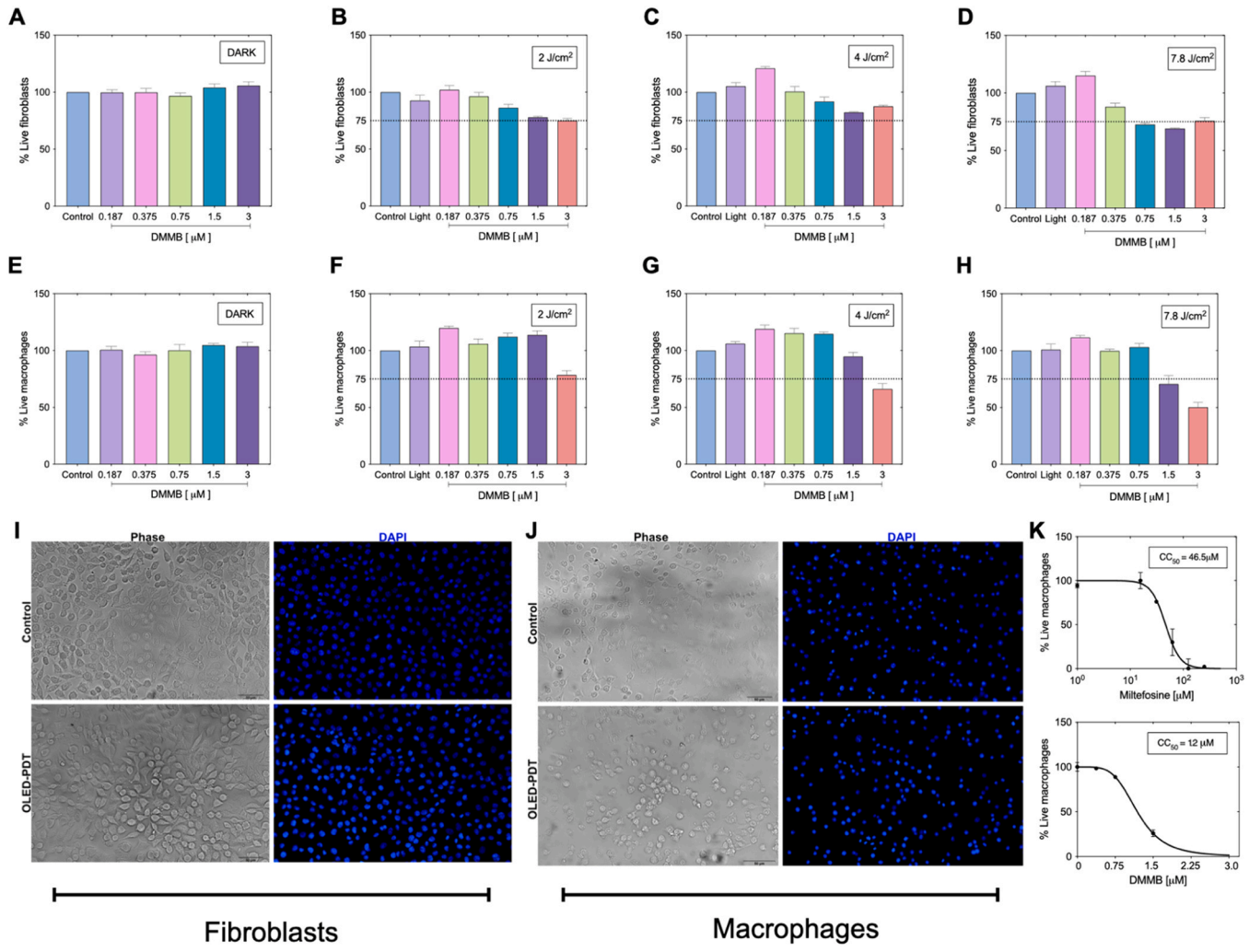

Fig. 4. *In vitro* cytotoxicity assay of NIH 3T3 fibroblast (top) and RAW 264.7 macrophages (bottom) cells treated with increasing concentrations of DMMB (A,E) in the dark and at different radiant exposures (B,F) 2 Jcm^{-2}, (C,G) 4 Jcm^{-2}, (D,H) 7.8 Jcm^{-2}. Data are presented as mean values ± SEM. Fluorescence microscopy images of fibroblasts (I) and macrophages (J) treated with DMMB at 1.5 μM and a light dose of 7.8 Jcm^{-2}. Phase contrast and DAPI staining of untreated control and OLED-PDT. Scale bar = 50 μm. CC_{50} of macrophages treated with increasing concentrations of miltefosine (0–500 μM) and DMMB (0–3 μM) at 7.8 Jcm^{-2} (K).

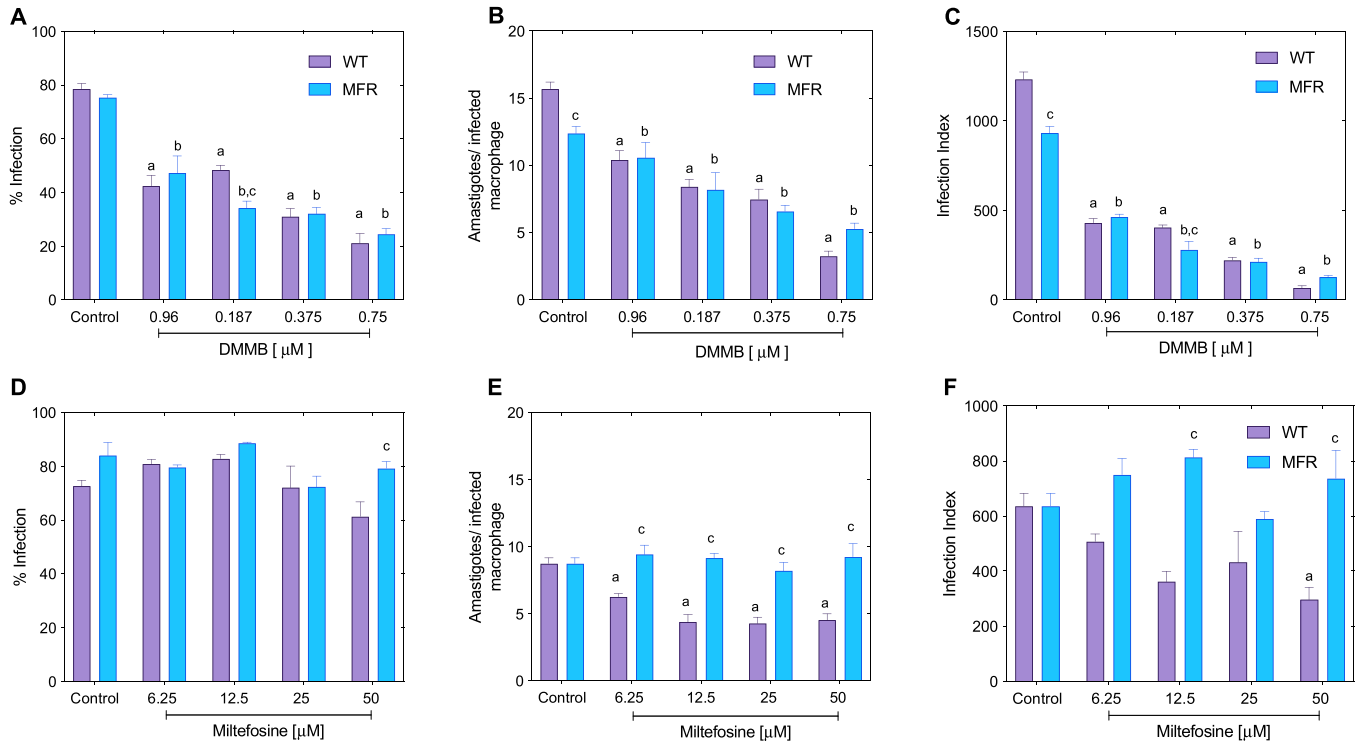

Fig. 5. The activity of OLED-PDT (0–0.75 μM) at 7.8 Jcm^{-2} and MF (0–50 μM) on intracellular amastigotes of *L. amazonensis* WT and MFR. Results were determined by counting 100 cells per coverslip and expressed as a percentage of infected macrophages and the average number of amastigotes per macrophage. Data are presented as mean values ± SEM. (A,D) Percentage of infection (B,E) Amastigotes per infected macrophage (C,F) Infection index. "a" denotes statistically significant differences between WT control and treated groups. "b" denotes statistically significant differences between MFR control and treated groups. "c" denotes statistically significant differences between WT and MFR.

concentration, the number of parasites was reduced by 34 % (from 15.7 to 10.4 in WT) and 15 % (from 12.3 to 10.5 in MFR). At a higher concentration (0.75 μM), OLED-PDT had a more pronounced effect, thus inactivating nearly 79.2 % (from 15.7 to 3.2) of the WT amastigotes, whereas about 42.6 % (from 12.3 to 5.2) of MFR parasites were killed under the same conditions (Fig. 5B and E).

When both parasites were treated with MF, there was a decrease of about 28 % in the number of WT parasites per infected cell (from 8.7 to 6.2) at the lowest DMMB concentration (6.25 μM), while at 50 μM, 48 % (from 8.7 to 4.5) of parasites were killed. However, MF exhibited no activity against the resistant parasites (Fig. 5E).

We also aimed to assess the infection index, which consists of the overall efficacy of the treatment. Our data show that the infection index was decreased by 65 % and 49.8 % at the lowest DMMB concentration (0.096 μM), while the killing rate was tremendously improved at 0.75 μM, reduced by 94.5 % and 86.3 % in the WT and MFR, respectively (Fig. 5C and F).

The infection index was significantly lower when the WT strain was treated with MF at 50 μM (53.3 %) compared to the untreated control. However, as expected, MF did not cause significant changes in the infection index in the MFR strain (Fig. 5F).

By using sigmoidal regression analysis, we calculated the EC_{50} related to the infection index of parasites treated with either MF or OLED-PDT. The EC_{50} values of MF for the MFR strain could only be calculated for conditions where there was an effect of the drug against this line. The MF EC_{50} value determined for the WT was 5.9 μM. When treated by OLED-PDT, the EC_{50} value found for the WT strain was 0.052 μM while for the MFR line, the EC_{50} was 0.077 μM. At the EC_{90} level, a different pattern was observed with values of 0.47 μM (WT) and 0.3 μM (MFR) (Fig. 6A).

According to these results, we calculated the SI. As shown in Table 2, the SI of MF for the WT was 7.7, while for MFR parasites it was very low (< 0.92). Surprisingly, OLED-PDT resulted in a much higher SI. It increased nearly 3-fold (22.5, WT) and 15-fold (15.3, MFR) when compared to MF.

We also assessed the levels of ROS and NO after OLED-PDT using the EC_{50} and EC_{90} values determined by each strain. The levels of ROS were raised by 57.9 % and 43.3 % when parasites were treated with a DMMB concentration corresponding to the EC_{50}. This effect was more pronounced when challenged with the EC_{90} concentration, hence resulting in about 100.4 % and 136.8 % increase for the WT and MFR lines, respectively (Fig. 6B).

In addition, to show the activation effects of OLED-PDT on infected macrophages, the levels of NO were measured over time for a 12-hour period. We demonstrated that OLED-PDT produced a stimulatory effect on macrophages infected by both strains. By calculating the area under the curve, we showed that OLED-PDT induced macrophages to generate 5 % and 7 % more NO when EC_{50} concentrations were used. NO production was greatly improved at a higher DMMB concentration (14 % and 12 % for the WT and MFR, respectively) (Fig. 6C and D).

3.4. In vivo evaluation of OLED-PDT and MF on BALB/c mice infected by L. amazonensis

For the initial *in vivo* study, BALB/c mice were infected subcutaneously in the left hind paw with late-stage promastigotes of *L. amazonensis* expressing the luciferase gene. Twenty-eight days post-infection, animals were randomly assigned into 2 groups; one group was the untreated control, and the other group was treated with OLED-PDT. Light parameters were set to deliver the same light dose (7.8 Jcm^{-2}) and intensity (6.5 $mWcm^{-2}$) used in the *in vitro* study. The DMMB concentration was established from the cytotoxicity assay. Therefore, it was applied subcutaneously at 1.5 μM concentration 10 min before irradiation. On day 0, animals received the first OLED-PDT session, being exposed to light for 20 min. Treatment was carried out 3 times a week for 2 weeks, totaling 6 sessions. Mice were monitored until day 21, 10

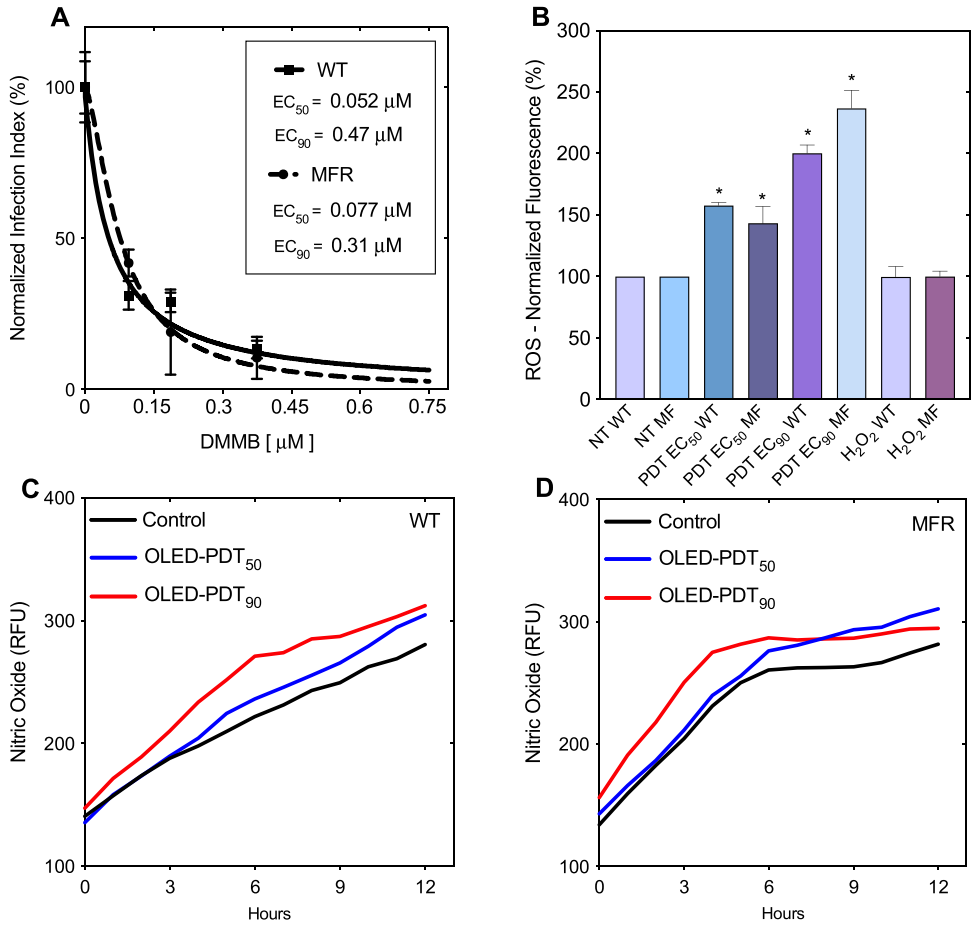

Fig. 6. Infection index dose-response curve, ROS and NO production on macrophages infected by intracellular amastigotes of WT and MFR *L. amazonensis*. (A) EC_{50} and EC_{90} of intracellular amastigotes of WT and MFR *L. amazonensis* treated with OLED-PDT at 7.8 Jcm^{-2}. (B) ROS detection after OLED-PDT. DMMB concentration corresponds to the EC_{50} and EC_{90} values of each strain. Data are presented as mean values ± SEM. * denotes statistically significant differences between WT and MFR treated groups and their respective untreated control. NO levels after OLED-PDT using DMMB at EC_{50} and EC_{90} values of (C) WT and (D) MFR strains. RFU: relative fluorescence units.

Table 2
EC_{50}, CC_{50} and selectivity index of intracellular amastigotes of WT and MFR *L. amazonensis* treated with MF and OLED-PDT at 7.8 Jcm^{-2}.

	MF Mφ	PDT Mφ	MF WT	MF MFR	PDT WT	PDT MFR
EC_{50} Ama/InfecMφ	N/A	N/A	5.9	> 50	0.052	0.077
CC_{50} Mφ	46	12	N/A	N/A	N/A	N/A
SI	N/A	N/A	7.7	< 0.92	22.5	15.3

Mφ = macrophages. Ama/InfecMφ = amastigotes per infected macrophage. MF and DMMB concentrations are expressed in μM. N/A: not applicable as CC_{50} is not applicable to parasites, and EC_{50} is not applicable to macrophages.

days after the end of the treatment. Parasite burden, lesion thickness, and pain sensitivity were also evaluated.

The results of OLED-PDT on infected BALB/c mice are displayed in Fig. 7. Since the *in vitro* studies demonstrated that DMMB at nanomolar concentrations were very effective against both lines, an initial study was performed to investigate whether the same light parameters and a low DMMB concentration (non-toxic to mammalian cells) would exhibit any efficacy on these animals. Unfortunately, however, our treatment did not demonstrate any statistically significant differences in parasite burden between the untreated control and OLED-PDT 1.5 group (Fig. 7A and B). Nevertheless, by the end of treatment lesion thickness was reduced by 32 % with significant differences compared to the control. Although on day 21 lesion thickness had increased, it was still 16 % smaller than the untreated group (Fig. 7C). Pain evaluation showed that treated animals were more tolerant to the nociceptive stimulus provoked at the end of the experiment, reduced by 50 % (Fig. 7D), thus suggesting that OLED-PDT had a positive impact on the clinical aspects of these animals. This can also be seen in the images shown in Fig. 7E, in which the untreated control had developed an ulcerated lesion by the end of treatment, while the treated group had none.

3.5. Increased PS concentration and combination therapy

In the second study, DMMB concentration was increased by 10 times to 15 μM (OLED-PDT 15), while light parameters were the same. We also aimed to investigate the potential of OLED-PDT 15 combined with a half dose of MF (6.5 MF). The drug combination is very advantageous for preventing the development of drug resistance. Therefore, OLED-PDT associated with MF could play a role in inhibiting the selection of resistant strains. In addition, dual therapy could reduce MF side effects. For this, BALB/c mice were infected and randomly sorted into 5 groups 28 days post-infection. There were 5 groups: (1) Untreated control, (2) OLED-PDT 15, (3) half dose of MF at 6.5 mg/kg/day (6.5 MF), (4) OLED-PDT 15 + 6.5 MF, (5) total dose of MF at 13 mg/kg/day (13 MF). MF was given orally for 15 consecutive days.

Our results demonstrate that a higher DMMB concentration (15 μM) significantly improved the efficacy of OLED-PDT even using the same light parameters, resulting in a nearly 1-log difference from untreated control by the end of the study. Most importantly, this remarkable result

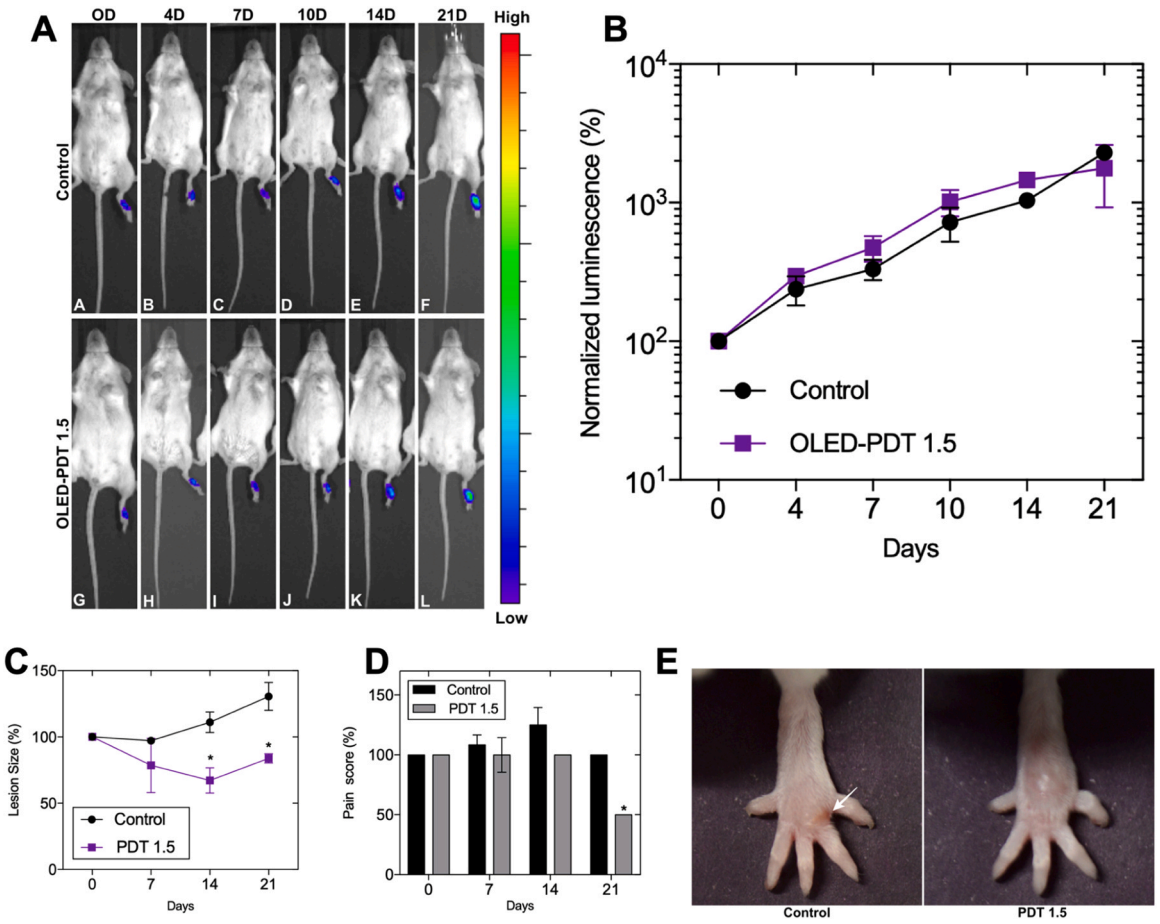

Fig. 7. OLED-PDT antileishmanial activity against *L. amazonensis* on infected BALB/c mice. (A) Bioluminescence images of untreated control and OLED-PDT 1.5 groups over time. The bar on the right side refers to a color scale representing light intensities expressed as ph/sec/cm^2/sr; (B) Parasite burden expressed in percentage as normalized luminescence; (C) Lesion thickness and (D) Pain score. Values represent means ± SEM. *denotes statistically significant differences between control and treated groups. (E) Clinical aspects of untreated control and OLED-PDT 1.5 groups 14 days post-treatment. The white arrow points to the ulcer developed through the course of infection.

was achieved by exposing infected mice to only 20 min of OLED irradiation, at a relatively low intensity (6.5 mWcm^{-2}) and light dose (7.8 J cm^{-2}). Although we did not notice a parasite burden reduction throughout treatment, OLED-PDT delayed parasite proliferation, while in the control group, an upward trend was shown (Fig. 8A and B). The same pattern was demonstrated for mice receiving 6.5 mg/kg of MF, hence suggesting those animals were exposed to sublethal doses of either OLED-PDT 15 or 6.5 MF.

In this context, the interaction of both therapies resulted in a tremendous impact on the parasite burden, which was reduced by 92 % after 14 days of treatment, resulting in approximately a 3-log difference from the untreated control. Remarkably, the parasite burden was completely eradicated at the end of the experimental period (day 21) and decreased by 98.5 % with a 4-log difference from the untreated group. It should be noted that such impressive result was sustained for at least one week after the end of treatment, suggesting that OLED-PDT potentiated the activity of MF, thus enabling us to reduce the dose by half, reaching similar results as the top dose (13 mg/kg) (Fig. 8A and B).

Lesion thickness was significantly reduced by 50 % in all treated groups after 7 days. By the end of treatment, only the groups treated with 13 mg/kg MF and the combination of both therapies showed a complete reduction in lesion thickness (Fig. 8C). Both groups treated with OLED-PDT showed a significant decrease in the pain score (by 33 %) in the first week of treatment, which was sustained over the entire course of the experimental period. Such improvement in the pain score was noticed only 14 and 21 days post-treatment in the groups receiving 13 and 6.5 mg/kg of MF, respectively (Fig. 8D).

Clinical aspects of animals are shown in Fig. 8E and F. By the end of treatment, we can see that the untreated control presented one large nodule that progressed to an ulcerated lesion in the following week (Fig. 8Ea and Fa). In addition, on day 21, another nodule appeared, thus suggesting that infection was not controlled in those animals (Fig. 8Fa). In contrast, all treated groups presented small lesion thicknesses without nodules or ulcerated lesions. It should be noted the presence of slight erythema in both OLED-PDT-treated groups at the end of treatment (defined by the redness across the skin), which disappeared on day 21 in the group treated with the combination of OLED-PDT 15 + 6.5 MF (Fig. 8Ed and Fd). However, although there was an improvement in the lesions of animals treated only with OLED-PDT 15, they still exhibited minor rashes over the surface of the skin at the end of the study (Fig. 8Eb and Fb). Despite that, the photosensitiser was well tolerated without significant signs of skin irritation. No necrosis or oedema was noticed in these mice.

4. Discussion

Herein, we show that OLED-PDT was effective in killing both strains of *L. amazonensis in vitro*. Moreover, for the first time, we demonstrate that OLED-PDT can be highly efficient in treating CL, mainly when combined with MF.

We found that OLED-PDT had minimal *in vitro* toxicity to mammalian cells depending on the light dose or DMMB concentration. Despite that,

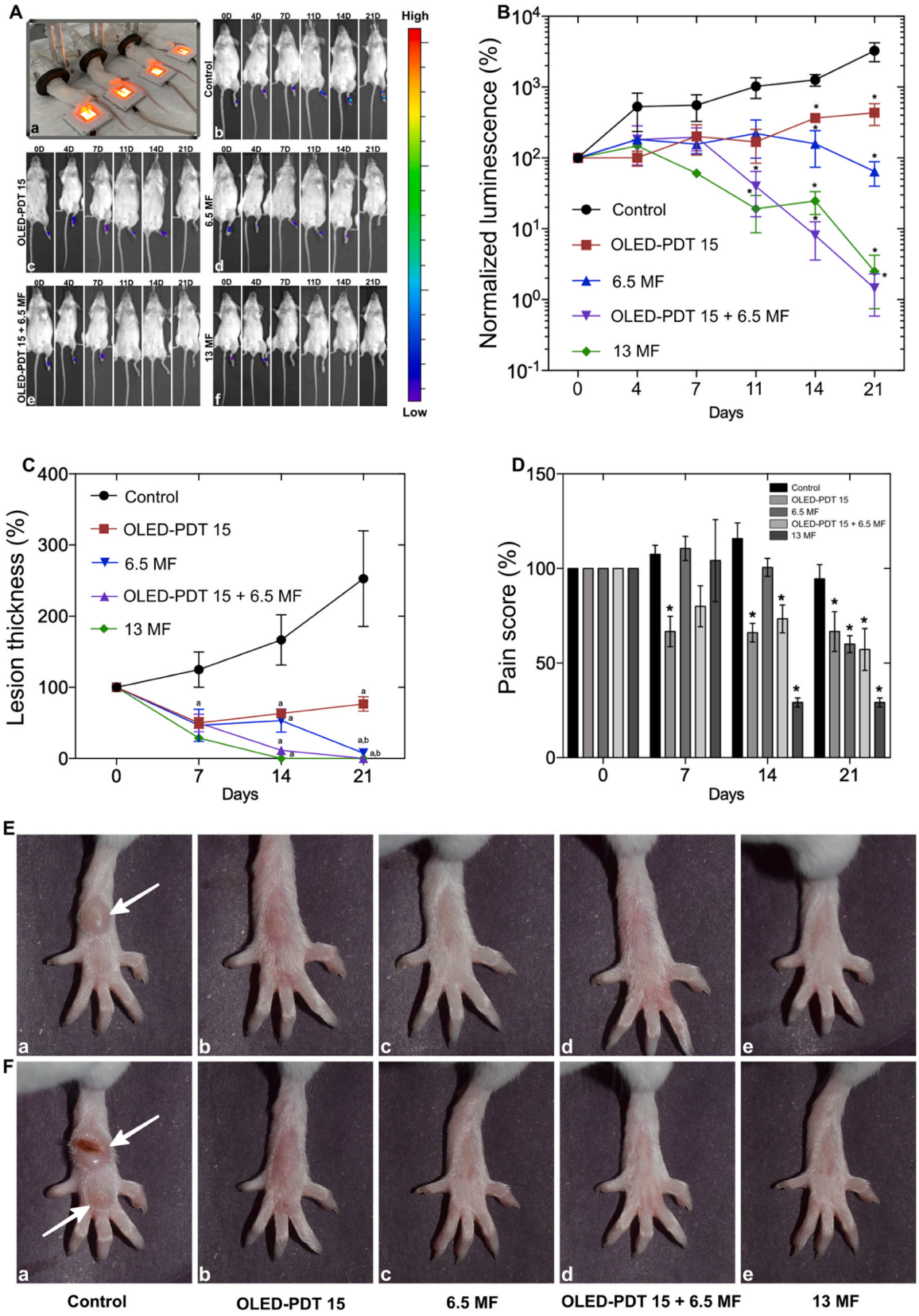

Fig. 8. OLED-PDT and MF antileishmanial activity against *L. amazonensis* on infected BALB/c mice. (A) Bioluminescence images of untreated control and treated groups over time. The bar on the right side refers to a color scale representing light intensities expressed as ph/sec/cm^2/sr; (B) Parasite burden expressed in percentage as normalized luminescence. Values represent means ± SEM. * denotes statistically significant differences between control and treated groups; (C) Lesion thickness and (D) Pain score. "a" denotes statistically significant differences between control and treated groups. "b" denotes statistically significant differences between OLED-PDT 15 and the other treated groups. Clinical aspects of untreated control and treated groups (E) 14 and (F) 21 days post-treatment. The white arrow points to the ulcer developed through the course of infection.

at the highest light dose (7.8 Jcm^{-2}), the OLED-PDT antileishmanial activity was increased nearly by 3-fold (WT) and 15-fold (MFR) compared to the standard oral drug MF (see Table 2). This result suggests that OLED-PDT has a highly selective activity against *Leishmania* over the host cells.

Indeed, this selectivity could be related to the higher affinity of DMMB for a lipid environment, thus easily diffusing across the lipid bilayer of cellular membranes [23,24]. In addition, such properties might increase the photosensitiser uptake by Leishmania-infected macrophages inside parasitophorous vacuoles (PVs) [25]. PVs are large compartments that protect parasites from oxidative stress, where they replicate within the cells. Therefore, the DMMB accumulation within PVs would generate significant amounts of ROS directly into the target, beyond parasites antioxidant defenses, thereby resulting in a high killing rate.

PDT has the advantage of dual selectivity, in which the photosensitiser can specifically reach intracellular organelles, and yet, light can be delivered directly onto the desired area, thus improving the efficacy of the therapy [8]. Moreover, PDT is very unlikely to select resistant strains [26]. The multi-target characteristics of PDT make this therapy attractive for the treatment of unresponsive patients, particularly those infected by resistant phenotypes.

Our results demonstrated that promastigotes and intracellular amastigotes of both WT and MFR were very susceptible to OLED-PDT. One possible reason can be attributed to the high levels of ROS produced. In addition, we found that OLED-PDT increased the levels of NO in infected macrophages after treatment. Indeed, parasite-host interactions play an important role in determining disease progression or cure. When macrophages are activated by a Th1-type immune response (M1 macrophages), pro-inflammatory cytokines stimulate macrophages to increase the production of ROS and NO, thereby resulting in parasite killing by oxidative damage [27]. Alternatively, a Th2-type immune response (M2 macrophages), inhibits the production of reactive species, thus contributing to parasite proliferation. In this regard, PDT mediated by chlorin e6 has been shown to polarize macrophages into an M1 phenotype [28]. We hypothesise that OLED-PDT might have activated M1 macrophages, therefore enhancing the amounts of NO produced.

According to the results *in vitro*, we determined the initial *in vivo* study. We decided to set the same light parameters and used a DMMB concentration that was not cytotoxic to mammalian cells. Despite the great results achieved *in vitro*, we found that those conditions were not sufficient to reduce the parasite burden on infected mice. Indeed, the infected tissue is a complex environment consisting of different epithelial cells and several biomolecules present in inflammatory exudates. Consequently, the photoactive drug can also bind to those biological components or be diluted by organic fluids [29]. Therefore, we assume the amounts of dye available to bind parasites were substantially reduced in the infected mice. Nevertheless, under these circumstances, we found a beneficial impact of OLED-PDT on lesion thickness and pain score. It has been shown that PDT can reduce lesion thickness and modulate the inflammatory responses of *Leishmania*-infected animals without significantly reducing parasite load, thus improving clinical healing, and relieving pain [30].

In the second part of the *in vivo* study, the DMMB concentration was increased by 10 times, achieving in 1-log difference in parasite burden from untreated control. Remarkably, such impressive results were accomplished at a relatively low intensity (6.5 $mWcm^{-2}$), light dose (7.8 Jcm^{-2}), and only 20 min of illumination each session. Importantly, the same light parameters used *in vitro* were suitable for our *in vivo* studies. This is particularly significant considering that previous studies using methylene blue and LEDs against *L. amazonensis* demonstrated that the light dose used *in vivo* (150 J cm^{-2}) to produce an effect over the parasite burden was 3 times higher than that used for *in vitro* experiments (50 Jcm^{-2}) [21]. Indeed, low light intensities might offer a further advantage [31]. PDT effects are thought to be dependent upon the oxygen supply, therefore high intensities and light doses (continuously delivered in one single session) can rapidly deplete molecular oxygen, thus compromising the efficacy of therapy [32]. Thus, by using low intensities and fractionated light doses (in our study 6 sessions) it is possible to allow reoxygenation of the tissue, hence improving the outcome.

On the other hand, *Leishmania* parasites can evade the host's immune response and survive even in harsh conditions [33]. Particularly *L. amazonensis*, which is one of the most prevalent species of CL, can develop a systemic and complex form of the disease, defined as diffuse CL. Our results show that under the given experimental conditions, OLED-PDT delayed parasite proliferation, but eventually, the remaining parasites could cause a relapse of the infection. Therefore, to prevent the development of more serious clinical manifestations, we aimed to associate OLED-PDT with a half dose of MF, the only oral drug available at present to treat leishmaniasis.

Drug combinations are advantageous for increasing the efficacy of the therapy, shortening the course of treatment, reducing costs, and preventing the emergence of resistance. Indeed, it has been reported that PDT combined with antibiotics appears to be a promising strategy to tackle drug resistance in bacterial infections [34]. Likewise, the interaction of OLED-PDT with a half dose of MF resulted in a substantial parasite burden reduction, achieving a 4-log difference compared to the untreated group. This extraordinary result caused a complete eradication of parasite load and a reduction in lesion thickness at the end of the study. Indeed, it is well-known that BALB/c mice when infected by *L. amazonensis*, have predominantly a Th2 cell type immune response, meaning that they are unable to control infection if left untreated [35]. Thus, the results achieved were mostly caused by the given treatment.

Although the mechanism of action of MF is poorly understood, it has been suggested that this drug may interfere with the lipid metabolism of parasites [36]. In addition, MF has shown immunomodulatory effects by inducing the activation of Th1 cytokines, which are essential to control *Leishmania* infection due to enhanced production of ROS and NO by macrophages [36]. Yet, a Th1-type response can be improved when combined with other therapies or compounds. Indeed, we also observed an increase in NO production *in vitro* after irradiation, suggesting an M1 macrophage polarization. Therefore, we assume that OLED-PDT potentiated the activity of MF allowing us to reduce the dose by half.

Given the long half-life of MF, a lower dose of the drug might reduce side effects and systemic toxicity besides preventing the selection of resistant strains, hence improving patient compliance. We also show that OLED-PDT was well-tolerated by animals, making the OLEDs suitable for topical administration. This is particularly significant because OLEDs can be flexible and conformable to human skin, being ideal wearable light sources for medical applications. Therefore, in a combination regimen, minimal clinical monitoring would be needed, thus encouraging the widespread use of dual therapy for CL in ambulatory care.

In conclusion, we have successfully demonstrated for the first time the potential of OLED-PDT against both stages of two strains of *L. amazonensis*, including a drug-resistant line. Moreover, our results indicate that OLED-PDT is suitable for combination treatment with MF, offering a viable approach for at-home care and effectively combating the emergence of resistant strains in CL.

Ethics approval

Animal experimentation was approved by the Ethical Committee on Animal Use from IPEN-CNEN under the protocol number 280/21.

CRediT authorship contribution statement

Fernanda Cabral: Investigation, Conceptualization, Data curation, Writing - original draft. **Mina Riahi:** Formal analysis, Data curation. **Cheng Lian:** Investigation. **Saydulla Persheyev:** Investigation. **Mauro Cortez:** Investigation. **Ifor Samuel:** Writing - Review & editing,

Supervision, Project Administration, Conceptualization. **Martha Ribeiro:** Writing - review & editing, Supervision, Project Administration, Conceptualization.

Declaration of Competing Interest

Competing Interests: I.D.W.S. is a founder and shareholder of Lustre Skin Ltd, which develops wearable light sources for the treatment of acne.

Data Availability

The research data underpinning this publication can be accessed at: http://doi.org/10.17630/4a90bd3a-623c-43df-a572-fbc6b1e54309.

Acknowledgements

We are grateful for funding from the Engineering and Physical Sciences Research Council of the UK (grants EP/R035164/1 and EP/L015110/1) and the Scottish Funding Council (ODA GCRF fund grant SFC/AN/12/2017). We also thank Photonics Institute (INFO) and SISFOTON from Conselho Nacional de Desenvolvimento Científico e Tecnológico (CNPq, grants #465763/2014–6 and 440228/2021–2) and Comissão Nacional de Energia Nuclear (CNEN).

Consent for publication

All authors have read and approved the manuscript, its content, and its submission to the Journal.

References

[1] M. Pires, B. Wright, P.M. Kaye, V. da Conceição, R.C. Churchill, The impact of leishmaniasis on mental health and psychosocial well-being: a systematic review, PLoS One 14 (2019) e0223313.
[2] S. Burza, S.L. Croft, M. Boelaert, Leishmaniasis. Lancet (Lond., Engl.) 392 (2018) 951–970.
[3] A. Ponte-Sucre, et al., Drug resistance and treatment failure in leishmaniasis: A 21st century challenge, PLoS Negl. Trop. Dis. 11 (2017) e0006052.
[4] T. Sunyoto, J. Potet, M. Boelaert, Why miltefosine—a life-saving drug for leishmaniasis—is unavailable to people who need it the most, BMJ Glob. Health 3 (2018) e000709.
[5] S. Palić, J.H. Beijnen, T.P.C. Dorlo, An update on the clinical pharmacology of miltefosine in the treatment of leishmaniasis, Int. J. Antimicrob. Agents 59 (2022) 106459.
[6] K. Seifert, S.L. Croft, In vitro and in vivo interactions between miltefosine and other antileishmanial drugs, Antimicrob. Agents Chemother. 50 (2006) 73–79.
[7] G.-J. Wijnant, et al., Tackling drug resistance and other causes of treatment failure in leishmaniasis, Front. Trop. Dis. 3 (2022) 837460.
[8] M.R. Hamblin, T. Hasan, Photodynamic therapy: a new antimicrobial approach to infectious disease? Photochem. Photobiol. Sci. 3 (2004) 436–450.
[9] C.P. Sabino, et al., Global priority multidrug-resistant pathogens do not resist photodynamic therapy, J. Photochem. Photobiol. B. (2020) 111893.
[10] A.B. Oliveira, T.M. Ferrisse, C.R. Fontana, F.G. Basso, F.L. Brighenti, Photodynamic therapy for treating infected skin wounds: a systematic review and meta-analysis from randomized clinical trials, Photo Photo Ther. 40 (2022) 103118.
[11] D.B. Hormazábal, et al., Synergistic effect of Ru(II)-based type II photodynamic therapy with cefotaxime on clinical isolates of ESBL-producing *Klebsiella pneumoniae*. Biomed. Pharm. 164 (2023) 114949.
[12] Y.H. Hsieh, et al., An in vitro study on the effect of combined treatment with photodynamic and chemical therapies on *Candida albicans*, 24, Int J. Mol. Sci. 19 (2) (2018) 337.
[13] M.R. Ronqui, T.M. de Aguiar Coletti, L.M. de Freitas, E.T. Miranda, C.R. Fontana, Synergistic antimicrobial effect of photodynamic therapy and ciprofloxacin, J. Photochem. Photobio. B 158 (2016) 122–129.
[14] A.R. Silva, et al., New insights in phenothiazinium-mediated photodynamic inactivation of *Candida auris*, J. Fungi. 9 (2023) 717.
[15] M. Wainwright, H. Mohr, Walker, H. W, Phenothiazinium derivatives for pathogen inactivation in blood products, J. Photochem. Photobiol. B. 86 (2007) 45.
[16] J.H. Sim, et al., OLED catheters for inner-body phototherapy: a case of type 2 diabetes mellitus improved via duodenal photobiomodulation, eadh8619, Sci. Adv. 9 (2023). eadh8619.
[17] S. Choi, et al., Wearable photomedicine for neonatal jaundice treatment using blue organic light-emitting diodes (OLEDs): toward textile-based wearable phototherapeutics, Adv. Sci. 9 (2022) 2204622.
[18] C. Lian, K. Yoshida, C. Nogues, I.D.W. Samuel, Organic light-emitting diode based fluorescence sensing system for DNA detection, Adv. Mater. Technol. 7 (2022) 2100806.
[19] A.C. Coelho, C.T. Trinconi, C.H.N. Costa, S.R.B. Uliana, In vitro and in vivo miltefosine susceptibility of a Leishmania amazonensis isolate from a patient with diffuse cutaneous leishmaniasis, PLoS Negl. Trop. Dis. 8 (2014) e2999.
[20] J.Q. Reimao, et al., Parasite burden in Leishmania (Leishmania) amazonensis-infected mice: validation of luciferase as a quantitative tool, J. Microbiol. Methods 93 (2013) 95–101.
[21] F.V. Cabral, et al., Preclinical investigation of methylene blue-mediated antimicrobial photodynamic therapy on Leishmania parasites using real-time bioluminescence, Photochem. Photobiol. 96 (2020) 604–610.
[22] M.V.P. De Sousa, C. Ferraresi, A.C. De Magalhães, E.M. Yoshimura, M.R. Hamblin, Building, testing and validating a set of home-made von Frey filaments: A precise, accurate and cost effective alternative for nociception assessment, J. Neurosci. Methods 232 (2014) 1–5.
[23] F.V. Cabral, et al., Organic light-emitting diodes as an innovative approach for treating cutaneous Leishmaniasis, Adv. Mater. Technol. 6 (2021) 2100395.
[24] I.O.L. Bacellar, et al., Membrane damage efficiency of phenothiazinium photosensitizers, Photochem. Photobiol. 90 (2014) 801–813.
[25] J. Wilson, et al., Control of parasitophorous vacuole expansion by LYST/Beige restricts the intracellular growth of Leishmania amazonensis, PLoS Pathog. 4 (2008) e1000179.
[26] F. Cieplik, et al., Antimicrobial photodynamic therapy - what we know and what we don't. Crit. Rev. Microbiol. 44 (2018) 1–19.
[27] P. Kaye, P. Scott, Leishmaniasis: complexity at the host-pathogen interface, Nat. Rev. Microbiol. 9 (2011) 604–615.
[28] T.T. Yu, et al., Chlorin e6-induced photodynamic effect polarizes the macrophage into an M1 phenotype through oxidative DNA damage and activation of STING, Front. Pharmacol. 13 (2022) 837784.
[29] M.R. Hamblin, T. Dai, Can surgical site infections be treated by photodynamic therapy? Photo Photodyn. Ther. 7 (2010) 134–136.
[30] F.V. Cabral, T.H. Souza, S. dos, F.P. Sellera, A. Fontes, M.S. Ribeiro, Towards effective cutaneous leishmaniasis treatment with light-based technologies. A systematic review and meta-analysis of preclinical studies, J. Photochem. Photobiol. B Biol. 221 (2021) 112236.
[31] X. Ragàs, et al., Photodynamic inactivation of Acinetobacter baumannii using phenothiazinium dyes: in vitro and in vivo studies, Lasers Surg. Med. 42 (2010) 384–390.
[32] B.W. Pogue, T. Hasan, A theoretical study of light fractionation and dose-rate effects in photodynamic therapy, Radiat. Res. 147 (1997) 551–559.
[33] P. Scott, F.O. Novais, Cutaneous leishmaniasis: immune responses in protection and pathogenesis, Nat. Rev. Immunol. 16 (2016).
[34] Y. Feng, C. Coradi Tonon, S. Ashraf, T. Hasan, Photodynamic and antibiotic therapy in combination against bacterial infections: efficacy, determinants, mechanisms, and future perspectives, Adv. Drug Deliv. Rev. 177 (2021) 113941.
[35] E.R. Mears, F. Modabber, R. Don, G.E. Johnson, A review: the current in vivo models for the discovery and utility of new anti-leishmanial drugs targeting cutaneous leishmaniasis, PLoS Negl. Trop. Dis. 9 (2015) e0003889.
[36] S. Palić, P. Bhairosing, J.H. Beijnen, T.P.C. Dorlo, Systematic review of host-mediated activity of miltefosine in leishmaniasis through immunomodulation, Antimicrob. Agents Chemother. 63 (2019) e02507–e02518.